Fabrication of cross-linked starch-based nanofibrous mat with optimized diameter

ZAHRA ASHRAFI, SAEEDEH MAZINANI, ALI AKBAR GHAREHAGHAJI, AND LUCIAN LUCIA

ABSTRACT: The design and synthesis of natural and synthetic polymer blends have received recent and wide attention. These new biomaterials exhibit progress in properties required in the field of medicine and healthcare. Herein, the aim of present study is to fabricate starch (ST)/polyacrylic acid (PAA) electrospun nanofibrous mat with a smooth and uniform morphology, lowest fiber diameter (below 100 nm) and the highest possible starch content. Starch itself is poor in process-ability, and its electrospinning could be quite a challenging process. To address this, we carried out the response surface methodology (RSM) technique for modelling the electrospinning process. In order to have ST/PAA nanofibers with the finest possible diameter, optimized processing parameters (applied voltage, nozzle-collector distance and feed rate) obtained from RSM technique were applied. ST/PAA electrospun nanofibers with an average diameter of 74±13 nm were successfully achieved via the electrospinning method for the first time. The structure, preparation and properties of the nanofibrous structure were discussed. Results indicated that drug loaded ST/PAA blend nanofibrous structure has a great potential to be used in controlled drug release systems.

Application: This study shows the potential for processing and using starch for nanofiber structure.

There is a growing trend for better use of biopolymers and evolution of natural-synthetic hybrid materials [1-3]. Biopolymers are renewable resources that intrinsically exhibit antibacterial activity, biodegradability, and biocompatibility [4,5]. Starch is one of the most abundant and inexpensive nature-based polysaccharides. It is composed of two types of molecules: amylose, a linear or lightly branched (1→4)-linked α-glucopyranose, and amylopectin, a highly branched molecule of (1→4)-linked α-glucopyranose with α-(1→6) branch linkages. Starch has various amylose/amylopectin ratios, depending on its botanical source [6].

Studies with biocompatible starch-based polymers have recently earned great importance for use in several applications, such as filtration, textiles, and biomedical use. In the biomedical field, electrospun nanofibers are suitable for applications ranging from bone cement and bone replacement implants to tissue engineering scaffolds, drug delivery, and wound dressing [7-9]. Starch itself is challenging to process and in dimensional stability and mechanical properties. Therefore, pure starch is not directly applied. To improve the properties of starch, various physical or chemical modifications have been introduced [10-12].

Electrospinning is a highly versatile technique in terms of its cost effectiveness, simplicity, and controllability of fiber properties [13,14] The electrospinning of polysaccharides and their derivatives are limited to a few examples [2,15]. Complex polysaccharides from plant sources, such as starch, have not been completely electrospun into fine nanofibers because of the various chain conformations, poor solubility, and high surface tension [16]. Therefore, the productivity of the electrospinning process and fiber uniformity have remained a challenge [17,18]. Starch with higher amylose components shows better electrospinnability, but the high cost of it is an obstacle for scaled production [19].

Several published reports focus on starch nanofibers [20,21]. For instance, Kong et al. [22] have used the electro-wet-spinning method to fabricate pure starch fibers with average diameters in the order of micrometers. They used starch with high amylose content (about 80%) to get higher electrospinnability. Moreover, some toxic solvents, such as dimethyl sulfoxide, were used, which limit biomedical applications of the end product. In another work, Xu et al. [10] developed electrospun starch acetate nanofibers with 70% amylose content and different degrees of substitution. They evaluated the properties and performance of those nanofibers for drug delivery application. In a recent study, Tang et al. [16] fabricated synthetic ampicillin-starch-polymer composite nanofibers with an average diameter of 500 nm, which had some good characteristics for controlled drug release applications.

One effective technique for preparing new multipurpose electrospun nanofibers and overcoming the disadvantages of natural polymers is to blend biopolymers such as starch with a synthetic polymer such as polyacrylic acid (PAA) [23]. PAA is a non-toxic, water-soluble, biocompatible polymer with excellent mechanical properties [24]. It shows good compatibility with starch because of the high amount of carboxylic groups on its polymeric chain backbone.

To the best of our knowledge, we are the first to report on fabricating starch/polyacrylic acid (ST/PAA) nanofibrous mat.

In the first step, the present study focuses on the investigation of ST/PAA solution characteristics influencing the starch content and morphological control of the nanofibrous mat. In the second step, nanofibers diameter was minimized by using a response surface methodology (RSM) for processing parameters to obtain the high-performance superfine fibrous film. Finally, thermal cross-linking release profiles of metronidazole-loaded ST/PAA nanofibers were investigated.

EXPERIMENTS

Materials

Soluble starch, PAA (average Mv~450,000), and formic acid were obtained from Sigma-Aldrich Corporation (St. Louis, MO, USA). Metronidazole was purchased from Behvazan Pharmaceutical (Tehran, Iran). Distilled water was used in all the experiments. All chemicals were used as received.

Preparation of electrospun nanofibrous mat

Precise amounts of starch were dissolved in formic acid at concentrations of 5% (w/v). PAA solutions of 5% (w/v) were prepared by dissolving PAA in distilled water. The starch and PAA solutions were constantly stirred at room temperature for 24 h and 5 h, respectively, until homogeneous solutions were formed. The starch solution was mixed with the PAA solution at determined weight ratios. ST/PAA solutions were designated as SP-1, SP-2, SP-3, and SP-4 (S = starch; P = polyacrylic acid). The selected weight ratios of starch to PAA were 90:10, 80:20, 70:30, and 60:40, respectively. All solutions were well mixed for 10 h under moderate stirring to get homogenous mixtures. For drug-loaded samples, 1%, 3%, and 5% metronidazole was added to the solution and stirred at room temperature for several hours.

Nanofibrous layers were produced by electrospinning the blend solution. About 5 mL of as-prepared ST/PAA solution was put into a 10 mL syringe with a stainless steel needle (22G, length = 34 mm, outer diameter = 0.7 mm, inner diameter = 0.4 mm) and connected to the power supply, which could generate DC voltages in the range of 0–30 kV. The electrospun nanofibers were collected on aluminum foil under a determined distance from the syringe tip. A syringe pump was used to feed a constant amount of solution onto the tip.

Response surface methodology

RSM is a mathematical and statistical technique used to evaluate the relative significance of several independent parameters and predict optimum operating conditions for desirable responses [25,26]. The electrospinning process is affected by many parameters, classified broadly into solution, processing, and ambient parameters. However, simultaneous investigation of all parameters in a study would be impossible. The solution and processing parameters significantly affect the fibers' morphology; by proper manipulation of these parameters, we can get nanofibers of desired morphology and diameters.

In this study, we used the RSM technique based on the Box–Behnken design (BBD) to model the electrospinning process and conduct the experiments. The design of the experiment counted 17 runs. For each sample, the fiber diameter was recorded as a response under selected parameters of voltage (kV), nozzle-collector distance (cm), and feed rate (mL/h). We used Design-Expert Version 7.1.5 (Stat-Ease; Minneapolis, MN, USA) statistical software to determine the optimum values of the selected parameters for minimum nanofibers mean diameter and to plot the response surface graphs.

To obtain superfine fiber and desirable morphology at the same time, the effective ranges of processing parameters were selected after some preliminary experiments (**Table I**).

Measurements and characterization

The morphological behavior of electrospun ST/PAA mats was investigated using scanning electron microscopy (SEM, Philips XL-30) at an accelerating voltage of 25 kV, after being gold-coated. The diameter of the electrospun nanofibrous mat was measured using Image J software (National Institutes of Health; Bethesda, MD, USA). The average diameter, standard deviation, and diameter distribution of nanofibers were determined from 100 randomly selected fibers.

Thermal cross-linking

To render fibrous membranes insoluble in water, samples were heated under vacuum so that cross-linking was induced by esterification between the starch hydroxyl and PAA carboxylic groups. The fibrous membrane was heated at 120°C for 13 min, immersed in water for a day, and then dried for observation through a scanning electron microscope. Moreover, the Fourier transform-infrared (FTIR) spectroscopy spectra of ST/PAA nanofibers before and after the cross-linking were acquired with potassium bromide pellets on a Thermo Nicolet NEXUS 670 FTIR spectrometer (Thermo Fisher Scientific; Waltham, MA, USA) to survey the chemical characteristics of the samples.

Parameter	Low-level Actual	High-level Actual	Low-level Coded	High-level Coded
Voltage, A (kV)	13	20	–1	+1
Distance, B (cm)	10	20	–1	+1
Feed rate, C (ml/h)	0.5	1.5	–1	+1

I. Independent variables and their levels in coded and actual values.

Drug release profile

The drug release behavior of the metronidazole-loaded ST/PAA was studied in a phosphate-buffered saline solution with a pH of 7.4 at 37°C. The solutions were analyzed for drug concentration using a Shimadzu (Kyoto, Japan) UV-1700 ultraviolet spectrophotometer at a wavelength of 320 nm. The amount of released metronidazole was calculated as the difference between the initial and measured values of metronidazole in the nanofibrous layer. The released values were calculated according to a prepared standard curve.

RESULTS AND DISCUSSIONS

Morphology control

The initial aim of this study was to fabricate starch-based nanofibers with the lowest possible diameter and a defect-free smooth structure. As a first step, ST/PAA solutions with different ratios were electrospun under the same processing parameters (voltage at 16 kV, nozzle-collector distance at 15 cm, and feed rate at 0.5 mL/h) to control the morphological structure of the nanofibrous mat containing a high content of starch.

Figure 1 shows the SEM images of the electrospun nanofibers. For the ST/PAA ratio of 90:10, only irregular beads were collected (Fig. 1A). By increasing the amount of PAA in the electrospinning solution, more uniform nanofibers with spindle-like beads and lower bead densities were produced (Fig. 1B and 1C). The electrospinnability of the solution increased as the PAA to starch ratio increased. One possible explanation for this phenomenon is the decrease of the surface tension of the spinning solution caused by the ionizable side groups of PAA in a strong electrical field during electrospinning. In other words, PAA is an anionic polyelectrolyte that can respond to electric stimulus. It can increase the charge density on the surface of the jet. When the PAA content increased up to a 40% weight ratio of the blended solution, the beads disappeared and smooth fibers, in the absence of micro-phase separation (Fig. 1D), were produced, with an average diameter of 97±25 nm.

Diameter optimization of nanofibers

The electrospinning process is affected by many parameters, which were classified broadly into three categories: solution, processing, and ambient parameters. To optimize nanofiber diameters, we modeled the electrospinning process, with consideration of the most important parameters. Because sur-

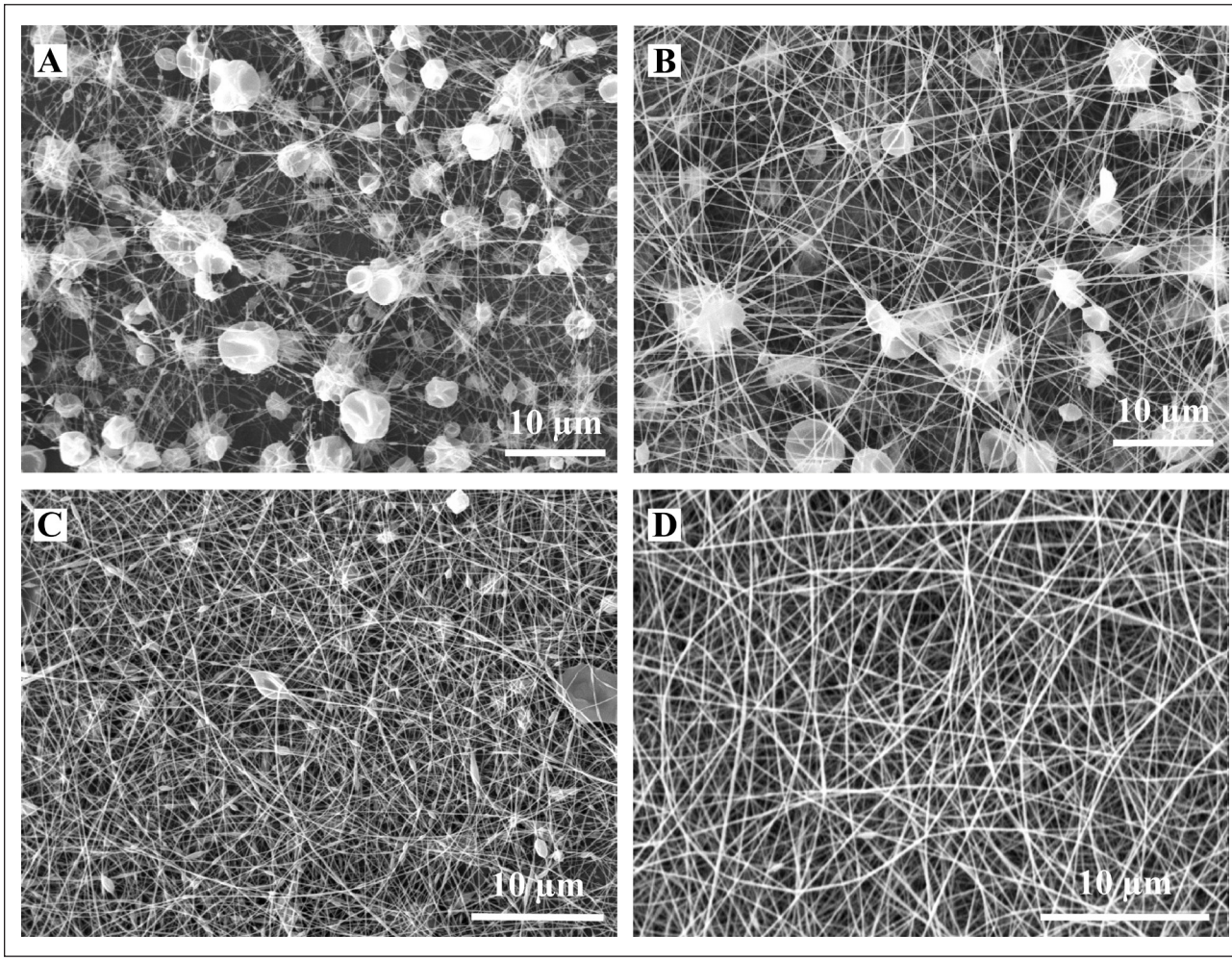

1. Scanning electron microscopy (SEM) photographs of electrospun nanofiber mats: A) SP-1, B) SP-2, C) SP-3, D) SP-4.

veying all of these parameters is almost impossible, only the influence of the most effective parameters can be investigated, while the other parameters are kept constant. Given that the solution parameters were optimized in the morphology optimization step, the processing parameters that showed the most important effect on the nanofibers diameter were applied voltage, needle-collector distance, and feed rate. These were selected as design variables. RSM based on the BBD as a multivariate technique was used to investigate the effects of these three independent parameters on the fiber diameter. The ranges of parameters were selected through visual control of electrospinning jet quality to attain the desirable morphology (Table I).

According to BBD with three factors, 17 experimental runs were designed. The designed experiments were performed, and the nanofibers diameter was considered as the modeling response. A quadratic regression mathematical model was developed for predicting the ST/PAA nanofibers diameter, statistical significance of each parameter, and their interactions. According to the analysis of variance (ANOVA), the model presented a high correlation coefficient ($R^2 = 0.9428$) and a non-significant lack of fit (0.2230), which indicated that the variation in the nanofibers diameter can reasonably be explained by the quadratic model. The modified regression equation (modified model) after removing the non-significant terms ($p > 0.05$) was obtained as Eq. 1:

$$D = 211.33578 - 7.41667 \times A - 9.43750 \times B + 4.70833 \times C + 0.50000 \times AB - 0.23333 \times AC \quad (1)$$

where D is the average ST/PAA nanofibers diameter (nm), A is applied voltage (kV), B is the needle-collector distance (cm), and C is the infusion rate (mL/h).

Eq. 1 suggests that all the selected parameters (applied voltage, nozzle-collector distance, and feed rate) play an effective role in determining the ST/PAA fibers diameter, and the applied voltage (A) is more important than the other parameters.

The optimum conditions for producing the nanofibers with minimum possible diameter were acquired by the modified model with an applied voltage of 19 kV, a needle-collector distance of 12 cm, and an infusion rate of 5 mL/h. The model predicts that nanofibers with a mean diameter of 72.54 nm could be formed under those conditions. Electrospinning under the optimized conditions produced nanofibers with mean diameter of 74±13 nm.

Figure 2 shows the SEM image of optimized nanofibers and the diameter distribution. The diameter was calculated exactly as a mean value of the 100 random measurements on the SEM micrographs. The optimized nanofibers were uniform and bead-free, with a cylindrical shape. **Table II** summarizes the data obtained from the experiments compared with data predicted by the model, and the results. The experimental values were reasonably close to the predicted ones. The low percentage of the absolute error for total designed experiments and the optimized nanofibers substantiates the accuracy and exactness of the modified model.

Effect of modeling variables

One of the advantages of using RSM is the evaluation of significance of each parameter and their interactions with the response variable. Previous related studies have not dealt with the modeling of the ST/PAA electrospinning process. **Figure 3** illustrates the importance of independent parameters and their interactions, which are quantified by means of ANOVA. Applied voltage and needle-collector distance both affect the nanofibers diameter inversely; that is, as these two parameters increase, the nanofibers diameter will decrease, whereas by increasing the infusion rate, the nanofibers diameter will increase.

Figure 4 shows counter-plots of the simultaneous effects of applied voltage/needle-collector distance and applied voltage/feed rate on the nanofibers diameter. The nanofibers di-

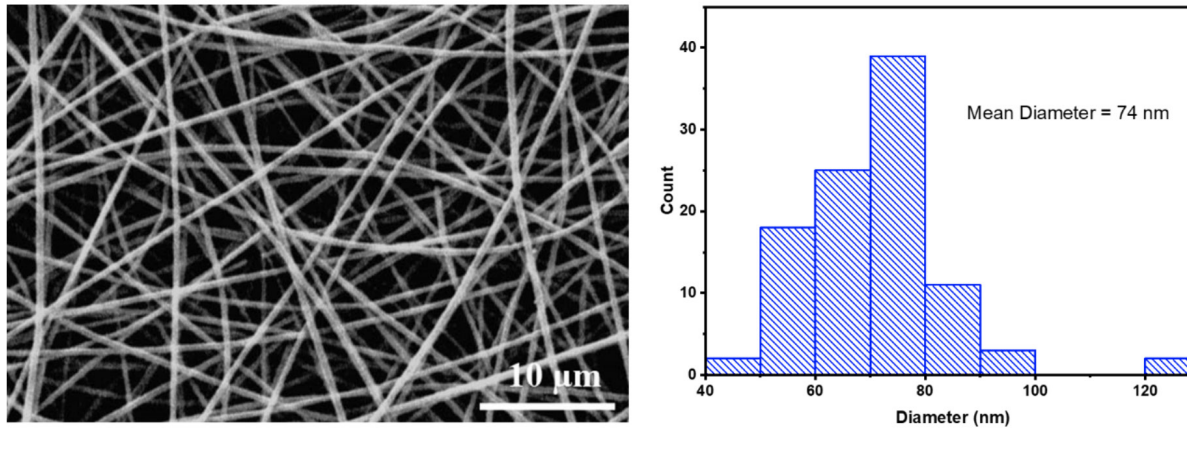

2. SEM images of selected starch/polyacrylic acid (ST/PAA) electrospun nanofibers (SP-4) with the optimum diameter and its diameter distribution at 19 kV power, 12 cm nozzle-collector distance, and 5 mL/h feed rate, respectively.

Run	A, kV	B, cm	C, ml/h	Experimental, nm	Predicted, nm	Absolute Error, %
1	16	14	1.0	82	82.29	0.36
2	16	12	1.5	87	90.04	3.50
3	13	14	0.5	83	82.17	1.00
4	19	14	1.5	77	78.42	2.05
5	16	14	1.0	82	85.29	0.36
6	13	16	1.0	83	84.67	2.01
7	16	16	0.5	87	98.54	3.19
8	16	12	0.5	81	80.29	0.87
9	19	12	1.0	76	73.92	2.74
10	19	14	0.5	72	72.67	0.93
11	13	14	1.5	101	110.92	2.06
12	16	14	1.0	83	82.29	0.85
13	13	12	1.0	98	96.42	1.61
14	19	16	1.0	73	74.17	1.60
15	16	14	1.0	79	82.29	4.17
16	16	16	1.5	86	84.29	1.98
17	16	14	1.0	80	83.29	2.87
Optimum Condition	19	12	0.5	74	72.54	1.97
Correlation Coefficient (R^2)						0.9428
Mean Absolute Percentage Error						1.90

II. The Box-Behnken design (BBD) matrix for three variables and response at different parameters' level for starch/polyacrylic acid (ST/PAA) nanofibers diameter.

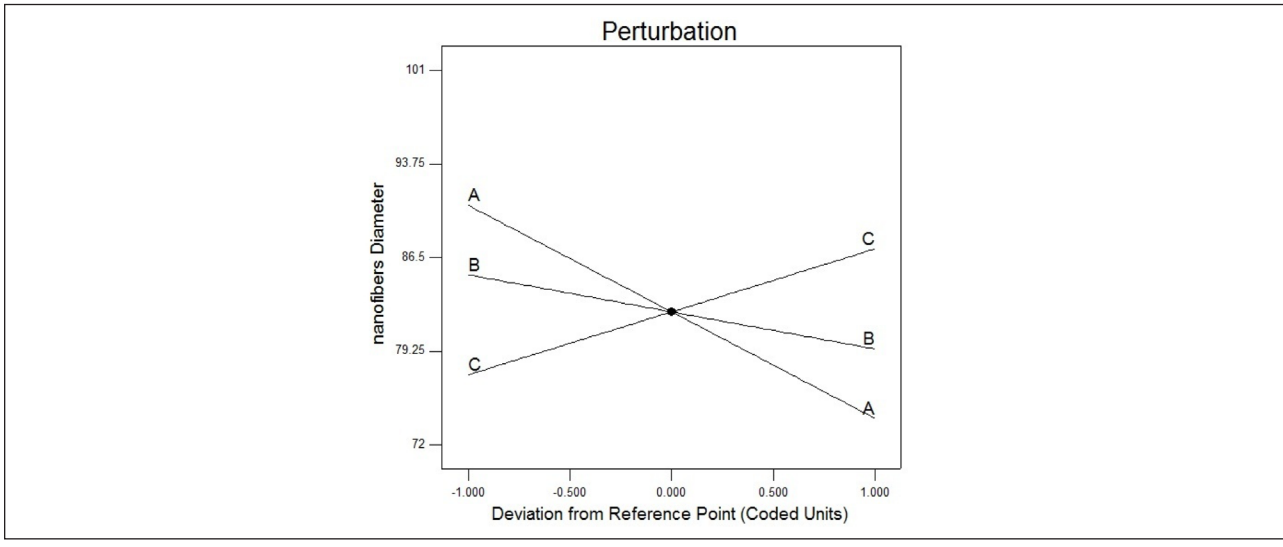

3. Perturbation plot of the parameters' effect on nanofibers diameter.

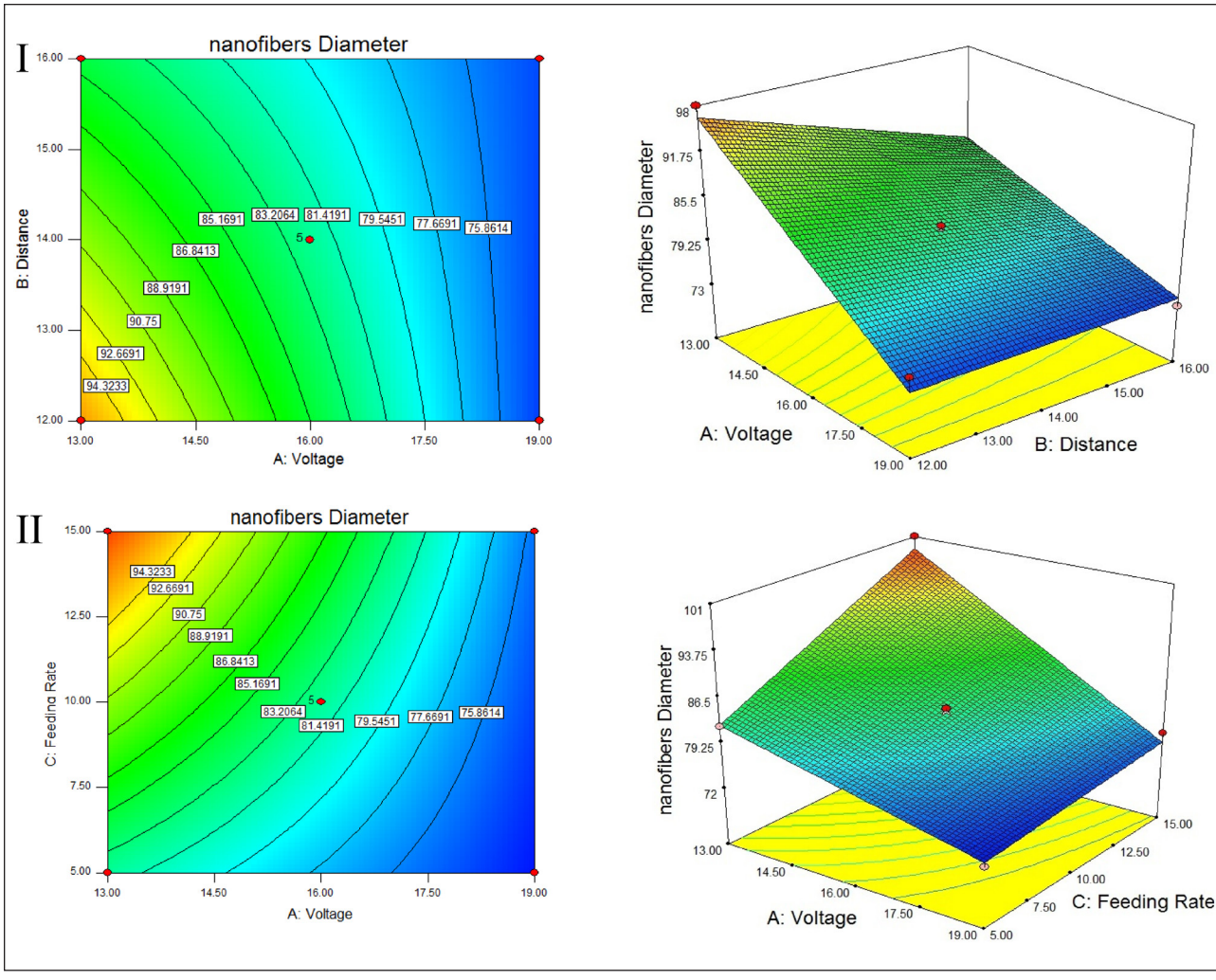

4. Plots of I) voltage and needle-collector distance interactions, and II) voltage and feed rate interactions.

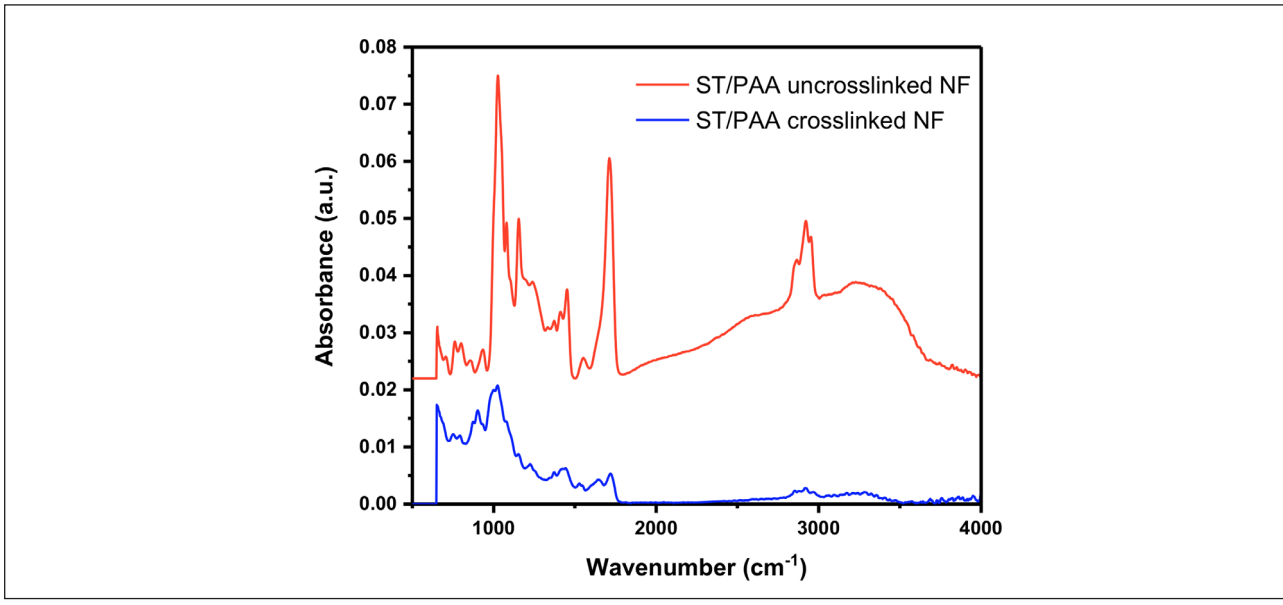

5. Fourier transform-infrared (FTIR) spectra of ST/PAA acid nanofibers before and after cross-linking.

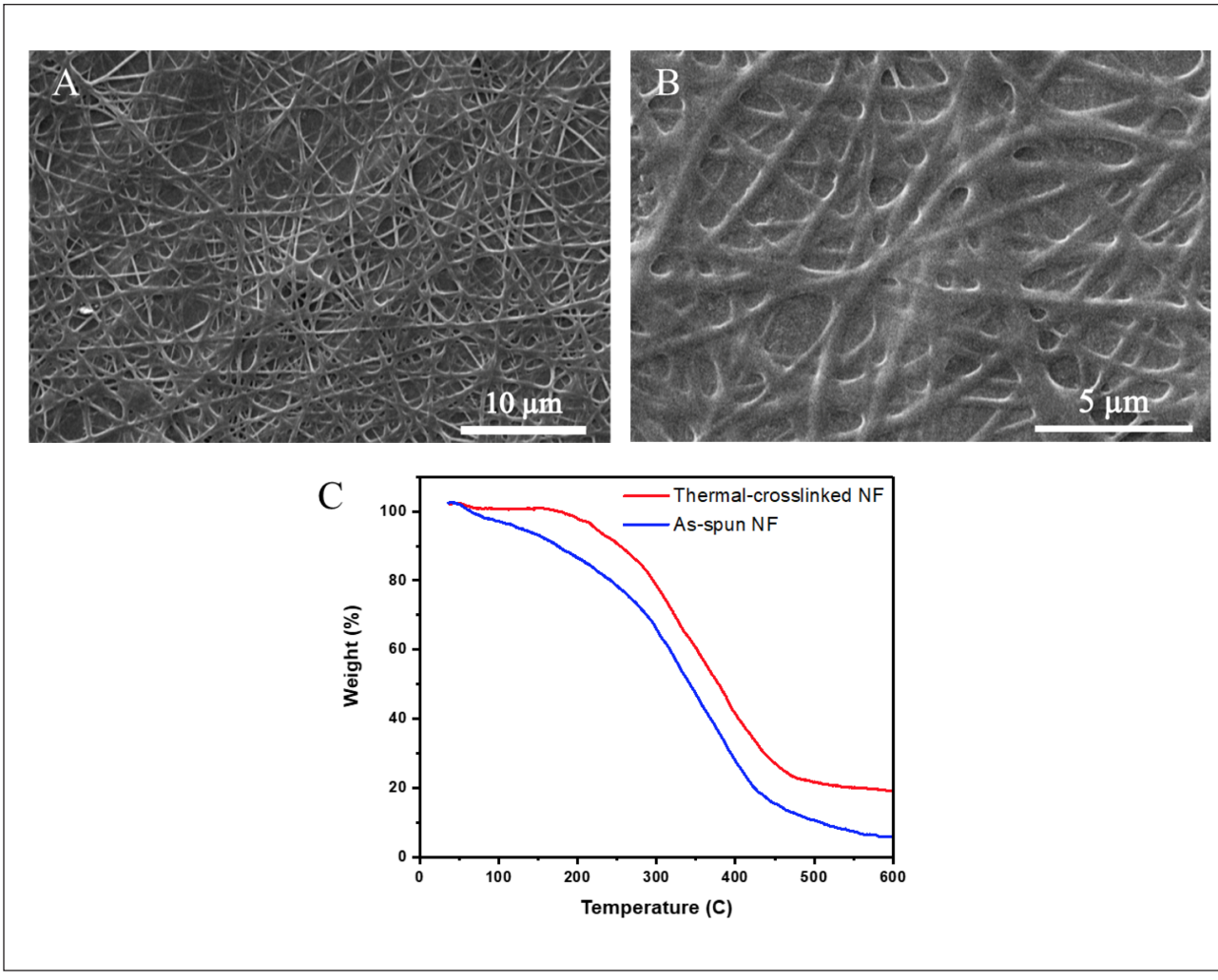

6. SEM images of cross-linked nanofibers after immersing in water for 10 h: A) scale bar 10 µm; B) scale bar 5 µm; C) thermogravimetric analysis (TGA) graph of as-spun and thermal crosslinked ST/PAA nanofibers; weight change as a function of temperature (20°/min).

ameter at a high level of feed rate (Fig. 4. II) and a low level of needle-collector distance (Fig. 4. I) are more responsive to the applied voltage variations. The figures suggest that the effect of applied voltage on the nanofibers diameter is more significant than that of other parameters.

Cross-linked nanofibrous structure

Ultra-fine ST/PAA fibrous structures instantly dissolve in aqueous media. To preserve their structure, samples were heated at 120°C for 15 min under vacuum to promote intermolecular cross-linking. We conducted FTIR and SEM studies on the treated samples to verify the sufficiency of the proposed method for cross-linking the ST/PAA nanofibers. **Figure 5** shows the FTIR spectra of the ST/PAA nanofibers in wave ranges of 500-4000 cm^{-1} before and after the cross-linking treatment.

The wide absorption band around 3400 cm^{-1} in the uncross-linked sample is attributed to the stretching vibration of the starch hydroxyl group. Uncross-linked nanofibers also show an intense absorption band caused by the carboxylic group of PAA at 1708 cm^{-1}. The FT-IR spectrum of the uncross-linked sample indicates that its blending with starch did not alter the absorbance of the carboxylic group peak, which was expected in the absence of esterification. However, in the spectrum of cross-linked nanofibers, the absorption band of the carboxylic group is weakened. In other words, during heating, carboxylic acid groups of PAA react with the hydroxyl groups from starch by esterification to form the ester bonds and change into water insoluble material [27]. **Figure 6** (A and B) shows an SEM image of treated nanofibers after 10 h in water, which confirms the merit of the method for cross-linking the ST/PAA nanofibers.

The thermogravimetric analysis (TGA) curve was obtained for both samples before and after cross-linking (Fig. 6C). The cross-linking effect occurs by increasing the thermal stability by at least about 50°C at T50, demonstrating the success of the suggested procedure with the tested blend. The increase in thermal stability is observed for all TGA temperature ranges, which supports the FTIR and SEM results.

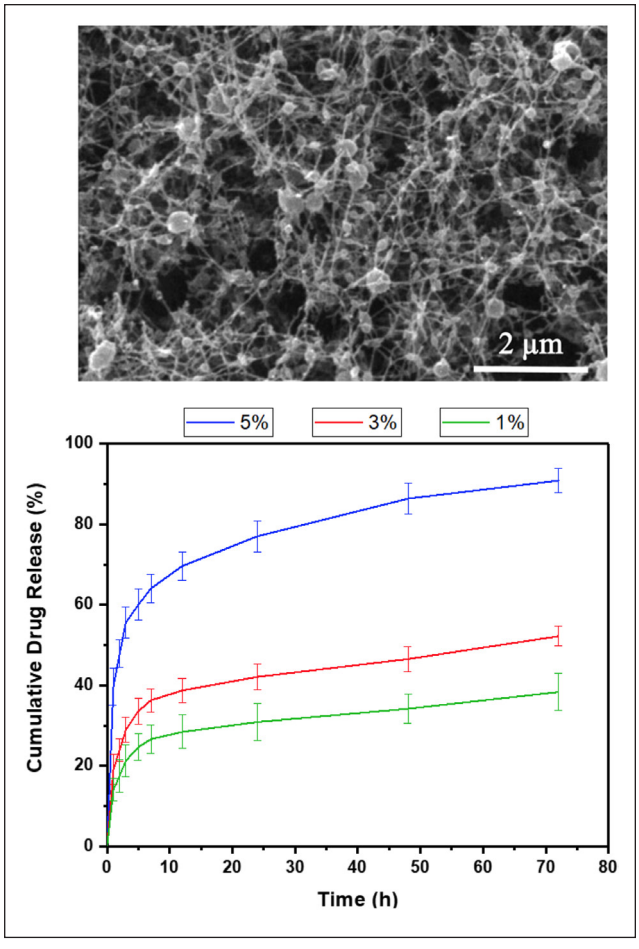

7. SEM image (top) of metronidazole-loaded ST/PAA nanofibers and plot (bottom) of percentage cumulative mass release profiles of different concentrations of metronidazole-loaded ST/PAA nanofibrous film over a span of 80 h.

Drug release profile

We have investigated the release profile of metronidazole from ST/PAA nanofibers containing 1%, 3%, and 5% metronidazole. **Figure 7** shows the metronidazole release profiles from ST/PAA nanofibrous mat after thermal cross-linking during 80 h of incubation in phosphate-buffered saline solution. After an initial burst of medication, all samples had a long period of smooth release (Fig. 7). As the metronidazole-loaded ST/PAA nanofibrous films are placed in an aqueous solution, water initially penetrates into the exposed surface of the nanofibers, and the metronidazole trapped within a thin surface layer is quickly released (the initial burst in Fig. 7). Subsequently, water penetrates more into the bulk of the nanofibers, causing polymer bond breakage and bulk erosion.

The main goals of this study were to fabricate starch-based nanofibers and find the optimized values of the electrospinning processing parameters to obtain the minimum diameter possible in the range of superfine fibers (below 100 nm). The diameter of the starch fibers produced by electrospinning is a key parameter that can give higher performance to a starch-containing nanofibrous mat in many applications. For instance, nanofibrous scaffolds with smaller diameters would provide better conditions for three-dimensional cell growth [27].

To the best of our knowledge, this is the first report on fabricating superfine ST/PAA nanofibers and its heat cross-linking. Although most polysaccharides are of fundamental interest for electrospinning and are useful in many applications, there are still limitations to overcome for electrospinning. Moreover, nanofiber membranes with higher surface area and porosity have higher ability to adsorb/absorb pollution, which makes them good candidates for applications such as wound dressing, drug release, and filtration.

CONCLUSIONS

Modeling and optimization of the electrospinning process were performed according to RSM designs, including 17 experimental runs. To minimize the average fiber's diameter, the applied model suggests using 19 kV power, 12 cm nozzle-collector distance, and 5 mL/h feed rate. Fiber diameters of 74±13 nm result using those settings. To prevent the dissolving of nanofibrous structure in aqueous media, heat cross-linking of nanofibers as a green method was successfully performed. FTIR, TGA, and SEM results showed the suitability of the proposed method for cross-linking the membrane. The blended nanofiber was used as a web for drug loading of metronidazole. The release profile results proved the acceptable role of nanofibers for drug release in this system. **TJ**

ACKNOWLEDGMENTS

This research was supported by Amirkabir University of Technology, Tehran, Iran.

LITERATURE CITED

1. Mazinani, S., Ajji, A., and Dubois, C., *J. Polym. Sci. Part B Polym. Phys.* 48(19): 2052(2010). https://doi.org/10.1002/polb.22085.
2. Sionkowska, A., *Prog. Polym. Sci.* 36(9): 1254(2011). https://doi.org/10.1016/j.progpolymsci.2011.05.003.
3. Ebrahimi, H., Najafi, F.S.A., Shahabadi, S.I.S., et al., *J. Compos. Mater.* 50(2): 269(2016). https://doi.org/10.1177/0021998315573560.
4. Schiffman, J.D. and Schauer, C.L., *Polym. Rev.* 48(2): 317(2008). https://doi.org/10.1080/15583720802022182.
5. Joghataei, M., Semnani, D., Salimpour, M.R., et al., *Int. J. Eng. Technol.* 5(1): (2016). https://doi.org/10.14419/ijet.v5i1.4853.
6. Srichuwong, S., Sunarti, T.C., Mishima, T., et al., *Carbohydr. Polym.* 60(4): 529(2005). https://doi.org/10.1016/j.carbpol.2005.03.004.
7. Liu, G., Gu, Z., Hong, Y., et al., *J. Controlled Release* 252: 95(2017). https://doi.org/10.1016/j.jconrel.2017.03.016.
8. Amini, M., Arash Haddadi, S., Ghaderi, S., et al., *Mater. Today: Proc.* 5(7, Part 3): 15613(2018). https://doi.org/10.1016/j.matpr.2018.04.170.
9. Zahedi, P., Rezaeian, I., Ranaei-Siadat, S.O., et al., *Polym. Adv. Technol.* 21(2): 77(2010). https://doi.org/10.1002/pat.1625.

10. Xu, W., Yang, W., and Yang, Y., *Biotechnol. Prog.* 25(6): 1788(2009). https://doi.org/10.1002/btpr.242.
11. Namazi, H., Fathi, F., and Dadkhah, A., *Sci. Iran.* 18(3): 439(2011). https://doi.org/10.1016/j.scient.2011.05.006.
12. Reis, A.V., Guilherme, M.R., Moia, T.A., et al., *J. Polym. Sci. Part A Polym. Chem.* 46(7): 2567(2008). https://doi.org/10.1002/pola.22588.
13. Kurtz, I.S. and Schiffman, J.D., *Materials* 11(7): 1059(2018). https://doi.org/10.3390/ma11071059.
14. Wang, G., Yu, D., Kelkar, A.D., et al., *Prog. Polym. Sci.* 75: 73(2017). https://doi.org/10.1016/j.progpolymsci.2017.08.002.
15. Lee, K.Y., Jeong, L., Kang, Y.O., et al., *Adv. Drug Delivery Rev.* 61(12): 1020(2009). https://doi.org/10.1016/j.addr.2009.07.006.
16. Kong, L. and Ziegler, G.R., *Biomacromolecules* 13(8): 2247(2012). https://doi.org/10.1021/bm300396j.
17. Stijnman, A.C., Bodnar, I., and Hans Tromp, R., *Food Hydrocoll.* 25(5): 1393(2011). https://doi.org/10.1016/j.foodhyd.2011.01.005.
18. Mendes, A.C., Stephansen, K., and Chronakis, I.S., *Food Hydrocoll.* 68: 53(2017). https://doi.org/10.1016/j.foodhyd.2016.10.022.
19. Hemamalini, T. and Giri Dev, V.R., *Int. J. Biol. Macromol.* 106: 712(2018). https://doi.org/10.1016/j.ijbiomac.2017.08.079.
20. Wang, H., Wang, W., Jiang, S., et al., "Poly(vinyl alcohol)/oxidized starch fibres via electrospinning technique: fabrication and characterization," *Iran. Polym. J.* 20(7): (2011).
21. Kong, L. and Ziegler, G.R., *Food Hydrocoll.* 38: 211(2014). https://doi.org/10.1016/j.foodhyd.2013.12.018.
22. Sunthornvarabhas, J., Chatakanonda, P., Piyachomkwan, K., et al., *Mater. Lett.* 65(6): 985(2011). https://doi.org/10.1016/j.matlet.2010.12.038.

ABOUT THIS PAPER

Cite this article as:
Ashrafi, Z., Mazinani, S., Gharehaghaji A., et al., *TAPPI J.* 18(6): 381(2019).
https://doi.org/10.32964/TJ18.6.381

DOI: https://doi.org/10.32964/TJ18.6.381

ISSN: 0734-1415

Publisher: TAPPI Press

About this journal

23. Kong, L. and Ziegler, G.R., *Food Hydrocoll.* 36: 20(2014). https://doi.org/10.1016/j.foodhyd.2013.08.021.
24. Goins, A., Ramaswamy, V., Dirr, E., et al., *Biomed. Mater.* 13(1): 2018. https://doi.org/10.1088/1748-605X/aa8439.
25. Ghani, M., Rezaei, B., Ghare Aghaji, A., et al., *Adv. Polym. Technol.* 35(4): 428(2016). https://doi.org/10.1002/adv.21569.
26. Ghani, M., Gharehaghaji, A.A., Arami, M., et al., *J. Nanotechnol.* Article ID 278418, 2014. https://doi.org/10.1155/2014/278418.
27. Li, L. and Hsieh, Y.-L., *Polymer* 46(14): 5133(2005). https://doi.org/10.1016/j.polymer.2005.04.039.

ABOUT THE AUTHORS

We chose this topic because of our team's interest in the nanofiber, nanotechnology, and drug release fields of study. Although there are different works in this field of application (nanofibers in drug delivery systems), the proposed blended nanofiber manufacturing and application in this area is quite novel.

Electrospinning of starch was the most challenging aspect of this study, which was handled with blending and optimization by use of the RSM method. One of the most interesting aspects of the study was being able to fabricate such a complicated nanofiber structure with electrospinning and obtaining fibers of diameters less than 100 nm. The research enabled us to introduce a new biopolymer-based nanofiber for biomedical applications.

The nanofiber can be developed for future application of wound dressing or drug release in biomedical industries. Our next step is to improve this nanofibrous web for drug release and examine criteria for using the material for other drugs.

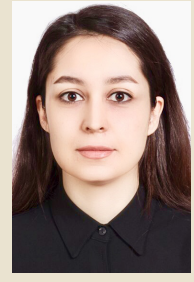

Ashrafi

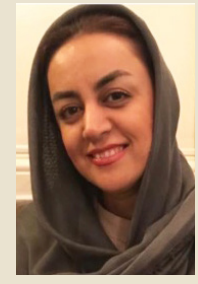

Mazinani

Gharehaghaji

Lucia

Ashrafi received her M.Sc. in Nanofibrous Structures Engineering from Amirkabir University of Technology (Polytechnic of Tehran), Tehran, Iran. At the time of submission of the current work, she was a Ph.D. student in the College of Textiles, North Carolina State University, Raleigh, NC, USA. Mazinani is faculty member, New Technologies Research Center (NTRC), Amirkabir University of Technology (Polytechnic of Tehran), Tehran, Iran. Gharehaghaji is faculty member, Department of Textile Engineering, Amirkabir University of Technology (Polytechnic of Tehran), Tehran, Iran. Lucia is professor, Department of Forest Biomaterials, North Carolina State University, Raleigh, NC, USA. Email Mazinani at s.mazinani@aut.ac.ir.